

# Improved Trial Wave Function for Quantum Monte Carlo Calculations of Nuclear Systems

Cody L. Petrie

January 25, 2017

## 1 Motivation

Understanding the interactions between nucleons has been a lengthy and difficult task to pursue for science. However, a thorough understanding of these interactions would give us great insight into the structure of nuclei and the formation of neutron stars [1, 2, 3, 4, 5]. Both of these areas of research are difficult to probe experimentally and would benefit greatly by good theoretical predictions to guide experiments in useful and exciting directions.

Despite the difficulty, science has been making continuous steps toward understanding these interactions, sometimes called the strong force. In 1935 Hideki Yukawa proposed the idea that this interaction, called the strong force, was governed by quanta or exchange particles [6]. These particles were later called pions [7]. He used what is now called the Yukawa potential, which is still used in modified form in many nuclear models today, to describe these interactions. The range of the force proposed by Yukawa was inversely proportional to the mass of the pion, and the strength of the force was based only on the distance separating the particles. Today we often use potentials that depend on the separation distance between the particles, but also their relative spins and isospins. These interactions can be quite complicated, making a true understanding of the strong force difficult to achieve.

Currently it is believed that Quantum Chromodynamics (QCD) is the most correct theory to describe the strong force [8]. However, due to asymptotic freedom at low energies, this theory becomes quite difficult to use and so other, approximate methods are often used to study the strong interaction.

A set of approximate methods called basis set methods are currently used to solve for properties of nuclei. Some of these methods are the no core shell model [9, 10], the coupled-cluster method [11] and the self-consistent Green's function method [12, 13]. For these methods the wave function of the nuclear system is written in terms of a truncated basis, often a harmonic oscillator basis. The momentum cutoff of the basis needs to be higher than the momentum of the interaction that is being used, in order to do calculations in momentum space. This means however that calculations with sharp potentials (like hard wall potentials) are difficult to do with basis set methods. They do employ techniques such as Similarity Renormalization Group [14] to soften these types of interaction. This allows them to decrease the number of basis functions used. One of the advantages of basis set methods is that they can use local and non-local, i.e. velocity dependent, potentials. The

Quantum Monte Carlo (QMC) methods, which I am using in this work, complement these basis set methods. Though they are currently limited to mostly local potentials [15], they do not have the momentum cutoff limits of the basis set methods and so can employ potentials with high momentum cutoff's.

Using these approximate methods to study nuclear systems will allow us to better understand the interactions between nuclei and ultimately will advance our understanding of many important processes in the universe.

## 2 Methods

There are a variety of methods that are used to solve the nuclear many-body problem. The most correct method that we know of is QCD, however it is often too difficult at low energies to solve problems with QCD due to asymptotic freedom [16, 17]. As a result many of the methods that are used to solve nuclear many-body problems are approximate methods. The methods that I will be using and describing in the following sections is the Quantum Monte Carlo (QMC) method [18].

Many methods that use the variational principle, QMC, often start with a trial wave function similar to the one used in Hartree-Fock [19], sometimes with Jastrow-like correlations [20]. However, to get an upper bound on energies they usually have to solve some sort of differential equation or multi-dimensional integrals. Especially if complicated spin-isospin dependent correlations are applied to the trial wave function, these integrals can be quite difficult to solve. Quantum Monte Carlo calculations use statistical sampling to solve large integrals that would otherwise be intractable. There are many good resources from which to learn about the many different QMC methods, [18, 21, 22, 23]. Here I will describe the methods that I have used in this research, those being Variational, Diffusion, and Auxiliary Field Diffusion Monte Carlo methods. Before describing those methods I am going to introduce the ideas of Monte Carlo integration and the Metropolis algorithm. Both of these tools will be used in the various QMC techniques.

### 2.1 Monte Carlo Integration

I will illustrate Monte Carlo Integration by imagining that we want to integrate the function  $g(\mathbf{R})$  where  $\mathbf{R} = \mathbf{r}_1, \mathbf{r}_2, \dots, \mathbf{r}_n$ , so

$$I = \int g(\mathbf{R}) d\mathbf{R}. \quad (1)$$

We can rewrite this integral in terms of a probability density called an importance function  $P(\mathbf{R})$ , and  $f(\mathbf{R}) = g(\mathbf{R})/P(\mathbf{R})$ .

$$I = \int f(\mathbf{R}) P(\mathbf{R}) d\mathbf{R} \quad (2)$$

This integral looks like the expectation value of  $f(\mathbf{R})$  as long as the  $\mathbf{R}$ 's are distributed according to  $P(\mathbf{R})$ . Thus we can find the integral by finding the expectation value. One way

to do that would be to take an infinite number of sample configurations from the importance function and evaluate the average of  $f(\mathbf{R})$  given that infinite set of samples.

$$I = \lim_{N \rightarrow \infty} \frac{1}{N} \sum_{n=1}^N f(\mathbf{R}_n) \quad (3)$$

Since we can't take an infinite number of samples we can approximate the integral by taking a large number of samples and finding the an approximate expectation value from that finite set.

$$I \approx \frac{1}{N} \sum_{n=1}^N f(\mathbf{R}_n). \quad (4)$$

This method of integration is useful especially when the dimensions of the integration increase. In many-body quantum mechanics the dimension of the integrals can be quite large, including several dimensions for each particle in the calculation. Monte Carlo Integration only needs to sample each of these dimension decreasing the work required by a substantial amount.

## 2.2 Metropolis Algorithm

Let's assume that we are doing Monte Carlo Integration as described above, but the importance function,  $P(\mathbf{R})$ , from which the random variables  $\mathbf{R}$  are drawn is a simple invertible function. We can then simply generate a random variable from the uniform distribution,  $u$ , and then figure out what value of  $x$  gives us that value given  $P(x) = u$ . This works quite well assuming the function  $P(x)$  is invertible. But let's say that we can't invert it. This is where the Metropolis algorithm comes in, allowing us to get random samples from  $P(x)$  even if it's non-invertible. The Metropolis algorithm is a Markov Chain method that uses only the previous point to determine where the next move will be, i.e. the step doesn't depend on history other than the previous step. These are the steps to the algorithm.

1. Start at a random position,  $\mathbf{R}$ .
2. Propose a move to a new position  $\mathbf{R}'$ , pulled from a distribution  $T(\mathbf{R}'|\mathbf{R})$ , where  $T$  can be a Gaussian centered on the current position. This makes sure that too large of steps aren't taken.
3. The probability of accepting the move is given by

$$A(\mathbf{R}'|\mathbf{R}) = \frac{P(\mathbf{R}')}{P(\mathbf{R})} \quad (5)$$

4. If  $A \geq 1$ , then the move is accepted. Otherwise a random number,  $u$ , is generated from a uniform distribution between 0 and 1, and the move is accepted if  $A > u$ .

## 2.3 Variational Monte Carlo

Variational Monte Carlo (VMC) starts with a trial wave function,  $\psi_T$ , that should have some non-zero overlap with the actual ground state wave function, and a Hamiltonian,  $\hat{H}$ . The expectation value of the Hamiltonian in the trial state gives what is called the variational energy. By the variational principle this energy is guaranteed to be an upper bound on the true ground state wave function.

$$E_V = \frac{\int \psi_T^*(\mathbf{R}) \hat{H} \psi_T(\mathbf{R}) d\mathbf{R}}{\int \psi_T^*(\mathbf{R}) \psi_T(\mathbf{R}) d\mathbf{R}} \leq E_0 \quad (6)$$

We want to do this integral using Monte Carlo integration and so we need it to look like equation 2. One way to get it into this form is to multiply the top integrand by  $\psi_T(\mathbf{R})\psi_T^{-1}(\mathbf{R})$  which gives

$$E_V = \int P(\mathbf{R}) E_L(\mathbf{R}) d\mathbf{R}, \quad (7)$$

where  $P(\mathbf{R}) = |\Psi_T(\mathbf{R})|^2 / \int |\Psi_T(\mathbf{R})|^2 d\mathbf{R}$  is the importance function and  $E_L(\mathbf{R}) = \Psi_T^{-1}(\mathbf{R}) \hat{H} \Psi_T(\mathbf{R})$  is called the local energy.

Now using the metropolis algorithm we can draw a set of random configurations,  $\{\mathbf{R}_n : n = 1, N\}$  from the probability distribution  $P(\mathbf{R})$  and use those to sample the local energy. These random configurations are called walkers and contain the positions as well as spins and isospins of each particle. The variational energy is then approximated by the expectation value of those samples.

$$E_V \approx \frac{1}{N} \sum_{n=1}^N E_L(\mathbf{R}_n). \quad (8)$$

At this point certain parameters in  $\Psi_T$  can be varied until a minimum in the energy is found. A minimum in the energy will be produced when  $\Psi_T \rightarrow \Psi_0$ . It is important to note however that the trial wave functions that we often use are not exactly the ground state wave functions and so the energies that we produce are only the minimum energy for that specific trial wave function. That is why it is important to start with the best trial wave function possible.

## 2.4 Diffusion Monte Carlo

Diffusion Monte Carlo (DMC) solves for the ground state by letting the walkers diffuse in imaginary time. You start with the Schrödinger equation

$$\hat{H}\Psi = i\hbar \frac{\partial \Psi}{\partial t}. \quad (9)$$

Now we substitute time for imaginary time using  $\tau = it/\hbar$  and notice that this looks similar to the diffusion equation.

$$\hat{H}\Psi = -\frac{\partial \Psi}{\partial \tau} \quad (10)$$

At this point we assume that the solution will consist of exponentials, but we shift the energies by a parameter,  $E_0$  that we can use to control the normalization,  $V \rightarrow V - E_0$  and  $E_n \rightarrow E_n - E_0$ .

$$\Psi(\mathbf{R}, \tau) = \sum_{n=0}^{\infty} c_n \phi_n(\mathbf{R}) e^{-\tau(E_n - E_0)} \quad (11)$$

Then one of the key parts of DMC is that as you let  $\tau \rightarrow \infty$  all of the states higher than the ground state die because the difference  $E_n - E_0$  is non-zero and the infinite  $\tau$  kills the exponential. This leaves only the ground state.

$$\lim_{\tau \rightarrow \infty} \Psi(\mathbf{R}, \tau) = c_0 \phi_0(\mathbf{R}) \quad (12)$$

Since we cannot generally compute this limit,  $\lim_{\tau \rightarrow \infty} \Psi(\mathbf{R}, \tau) = \lim_{\tau \rightarrow \infty} e^{(-H - E_0)\tau} \Psi(\mathbf{R})$ , directly we split the propagation into small steps in imaginary time. To do this let's write the propagated wave function and insert a complete set of states.

$$\langle \mathbf{R}' | \Psi_T(\tau) \rangle = \int d\mathbf{R} \langle \mathbf{R}' | e^{-(H - E_0)\tau} | \mathbf{R} \rangle \langle \mathbf{R} | \Psi_T(0) \rangle \quad (13)$$

Now you can break  $\tau$  up into  $N$  smaller time steps  $\Delta\tau = \tau/N$  and insert a complete set of states between each finite time propagator,

$$\langle \mathbf{R}_N | \Psi_T(\tau) \rangle = \int d\mathbf{R}_1 \dots d\mathbf{R}_N \left[ \prod_{i=1}^N \langle \mathbf{R}_i | e^{-(H - E_0)\Delta\tau} | \mathbf{R}_{i-1} \rangle \right] \langle \mathbf{R}_0 | \Psi_t(0) \rangle \quad (14)$$

$$= \int d\mathbf{R}_1 \dots d\mathbf{R}_N \left[ \prod_{i=1}^N G(\mathbf{R}_i, \mathbf{R}_{i-1}, \Delta\tau) \right] \langle \mathbf{R}_0 | \Psi_t(0) \rangle, \quad (15)$$

where  $\mathbf{R}_N = \mathbf{R}'$ ,  $\mathbf{R}_0 = \mathbf{R}$  and  $G(\mathbf{R}', \mathbf{R}, \tau) = \langle \mathbf{R}' | e^{-(H - E_0)\tau} | \mathbf{R} \rangle$ , is often called the Green's function or the propagator. It is often convenient to split up the kinetic and potential pieces of the Greens function into two parts. The kinetic term is used to move the walkers and the potential part is used to speed up convergence via a branching algorithm. The kinetic term gives us

$$G_0(\mathbf{R}', \mathbf{R}, \Delta\tau) = \langle \mathbf{R}' | e^{-T\Delta\tau} | \mathbf{R} \rangle, \quad (16)$$

which can be written as a diffusion term

$$G_0(\mathbf{R}', \mathbf{R}, \Delta\tau) = \left( \frac{m}{2\pi\hbar^2\Delta\tau} \right)^{3A/2} e^{-m(\mathbf{R}' - \mathbf{R})^2 / 2\hbar^2\Delta\tau}. \quad (17)$$

The piece that contains the potential then can be used to give a weight that gets used with the branching algorithm.

$$w(\mathbf{R}') = \langle \mathbf{R}' | e^{-(V - E_0)\Delta\tau} | \mathbf{R} \rangle \quad (18)$$

This sampling can give us large uncertainties and so we often use a function that does a good job describing the system (this can be the trial wave function) to guide the sampling.

This function is called an importance function,  $\Psi_I(\mathbf{R})$ , and thus the method is called importance sampling. The idea is that instead of sampling directly from the Green's function you will sample from

$$G(\mathbf{R}', \mathbf{R}, \Delta\tau) \frac{\langle \mathbf{R} | \Psi_I \rangle}{\langle \mathbf{R}' | \Psi_I \rangle}. \quad (19)$$

It turns out that this greatly improves the variance of the sampling. The DMC algorithm can generally be written as follows.

1. Generate a set of random walkers. These can be random or from a previously done VMC calculation.
2. For each walker propose a move,  $\mathbf{R}' = \mathbf{R} + \chi$ , where  $\chi$  is a random number from the shifted Gaussian  $\exp\left(\frac{m}{2\hbar^2\Delta\tau} \left(\mathbf{R}' - \mathbf{R} + 2\frac{\nabla\Psi_I(\mathbf{R}')}{\Psi_I(\mathbf{R}')}\right)^2\right)$ .
3. The move is then accepted with the probability  $P_{acc}(\mathbf{R}' \leftarrow \mathbf{R}) = \frac{\Psi_I^2(\mathbf{R}')}{\Psi_I^2(\mathbf{R})}$ .
4. For each walker calculate the weight  $w(\mathbf{R}') = \exp\left(-\left(\frac{E_L(\mathbf{R}') + E_L(\mathbf{R})}{2} - E_0\right)\Delta\tau\right)$ .
5. Do branching. This means that the number of copies for each walker that continues in the calculation is given by  $\text{int}(w(\mathbf{R}') + \chi)$ , where  $\chi$  is a uniform random number from  $[0, 1]$ . This way walkers with a small weight will more often be removed from the calculation and walkers with high weights will multiply.
6. Calculate and collect the observables and uncertainties needed and increase the imaginary time by  $\Delta\tau$ .
7. Repeat from step 2 to 6 until the uncertainties are small enough.

This method is described well in [18] and [23]. Green's function Monte Carlo (GFMC) and auxiliary field diffusion Monte Carlo (AFDMC) use this method to handle the spatial part of the calculation, but they each handle the spin part differently. Everywhere where the trial wave function is used in GFMC there is an explicit sum over the spin and isospin states. The number of possible spin states given  $A$  nucleons is  $2^A$ . The number of isospin states given  $A$  nucleons and  $Z$  protons can be reduced to  $\binom{A}{Z}$  states leaving us with a total of  $2^A \binom{A}{Z}$  spin-isospin states. The number of states increases quickly as the number of nucleons increases. As a result, to date, the largest nuclei that can be calculated with GFMC is  $^{12}\text{C}$ . As a result of this, AFDMC was developed as a way to use Monte Carlo methods to sample the number of states.

## 2.5 Auxiliary Field Diffusion Monte Carlo

To overcome the exponentially large number of spin-isospin states that have to be summed over in GFMC, AFDMC was developed in 1999 [22] to sample these states and, in analogy to moving the position of each walker, rotate the spin and isospin of each walker. To do this we use the basis where an element of the basis contains the three spatial coordinates of each

particle and the amplitude for each particle to be in each of the four possible spin-isospin states  $|s\rangle = |p \uparrow, p \downarrow, n \uparrow, n \downarrow\rangle$ . Now we need to write the spin-isospin dependent part of the propagator in this basis,

$$G_{SD}(R'S', RS, \Delta\tau) = \langle R'S' | e^{-V_{SD}\Delta\tau} | RS \rangle, \quad (20)$$

where  $V_{SD}$  does not include the central, non spin-isospin part of the potential. Here the potential can be written as

$$V_{SD} = \sum_{p=2}^M \sum_{i < j} v_p(r_{ij}) \mathcal{O}_{ij}^p, \quad (21)$$

where  $M$  is the number of operators that you use (e.g.  $M = 6$  for the  $v_6$  potential or  $M = 18$  for the Argonne  $v_{18}$  two-body potential [24]). In this study we have used the standard  $v_6$  potential which includes the operators  $\boldsymbol{\sigma}_i \cdot \boldsymbol{\sigma}_j$ ,  $\boldsymbol{\tau}_i \cdot \boldsymbol{\tau}_j$ ,  $\boldsymbol{\sigma}_i \cdot \boldsymbol{\sigma}_j \boldsymbol{\tau}_i \cdot \boldsymbol{\tau}_j$ ,  $S_{ij}$  and  $S_{ij} \boldsymbol{\tau}_i \cdot \boldsymbol{\tau}_j$ , where  $S_{ij} = 3\boldsymbol{\sigma}_i \cdot \hat{r}_{ij} \boldsymbol{\sigma}_j \cdot \hat{r}_{ij} - \boldsymbol{\sigma}_i \cdot \boldsymbol{\sigma}_j$ . Here the sigmas and taus are the pauli matrices applied to spin and isospin respectively. This potential can be written in the more convenient form

$$\begin{aligned} V_{SD} = & \frac{1}{2} \sum_{i,\alpha,j,\beta} \sigma_{i,\alpha} A_{i,\alpha,j,\beta}^\sigma \sigma_{j,\beta} \\ & + \frac{1}{2} \sum_{i,\alpha,j,\beta} \sigma_{i,\alpha} A_{i,\alpha,j,\beta}^{\sigma\tau} \sigma_{j,\beta} \boldsymbol{\tau}_i \cdot \boldsymbol{\tau}_j \\ & + \frac{1}{2} \sum_{i,j} A_{i,j}^\tau \boldsymbol{\tau}_i \cdot \boldsymbol{\tau}_j, \end{aligned} \quad (22)$$

where we have defined these new  $A$  matrices. These matrices are written in terms of the  $v_p(r_{ij})$  parameters above. For example the simplest matrix is the tau matrix which it is easy to see is  $A_{i,j}^\tau = v_\tau(r_{ij})$ . The half in equation 22 is because the sums are now over all particles  $i$  and  $j$  instead of over the pairs. These matrices are zero when  $i = j$  and they are symmetric. We can also write these matrices in terms of their eigenvalues and eigenvectors.

$$\sum_{j,\beta} A_{i,\alpha,j,\beta}^\sigma \psi_{n,j,\beta}^\sigma = \lambda_n^\sigma \psi_{n,i,\alpha}^\sigma \quad (23)$$

$$\sum_{j,\beta} A_{i,\alpha,j,\beta}^{\sigma\tau} \psi_{n,j,\beta}^{\sigma\tau} = \lambda_n^{\sigma\tau} \psi_{n,i,\alpha}^{\sigma\tau} \quad (24)$$

$$\sum_j A_{i,j}^\tau \psi_{n,j}^\tau = \lambda_n^\tau \psi_{n,i}^\tau \quad (25)$$

Written in terms of these eigenvalues and eigenvectors the potential can be written as

$$\begin{aligned} V_{SD} = & \frac{1}{2} \sum_{n=1}^{3A} (O_n^\sigma)^2 \lambda_n^\sigma \\ & + \frac{1}{2} \sum_{\alpha=1}^3 \sum_{n=1}^{3A} (O_{n\alpha}^{\sigma\tau})^2 \lambda_n^{\sigma\tau} \\ & + \frac{1}{2} \sum_{\alpha=1}^3 \sum_{n=1}^A (O_{n\alpha}^\tau)^2 \lambda_n^\tau, \end{aligned} \quad (26)$$

where the operators are given by

$$\begin{aligned}
O_n^\sigma &= \sum_{j,\beta} \sigma_{j,\beta} \psi_{n,j,\beta}^\sigma \\
O_{n\alpha}^{\sigma\tau} &= \sum_{j,\beta} \tau_{j,\alpha} \sigma_{j,\beta} \psi_{n,j,\beta}^{\sigma\tau} \\
O_{n\alpha}^\tau &= \sum_j \tau_{j,\alpha} \psi_{n,j}^\tau
\end{aligned} \tag{27}$$

These operators in the propagator now have the effect of rotating the spinors, analogous to diffusing the walkers in space. To reduce the order of the operators in the propagator from quadratic to linear we now use the Hubbard-Stratanovich transformation.

$$e^{-\frac{1}{2}\lambda\hat{O}^2} = \frac{1}{\sqrt{2\pi}} \int dx e^{-\frac{x^2}{2} + \sqrt{-\lambda}x\hat{O}} \tag{28}$$

The variable  $x$  is called an auxiliary field. Using the fact that there are  $3A$   $O_n^\sigma$  operators,  $9A$   $O_{n\alpha}^{\sigma\tau}$  operators and  $3A$   $O_{n\alpha}^\tau$  operators, for a total of  $15A$  operators, and by using the Hubbard-Stratanovich transformation we can write the spin-isospin dependant part of the propagator as

$$\prod_{n=1}^{15A} \frac{1}{\sqrt{2\pi}} \int dx_n e^{-\frac{x_n^2}{2}} e^{\sqrt{-\lambda_n} \Delta\tau x_n O_n}. \tag{29}$$

The spinors are then rotated based on auxiliary fields sampled from the Gaussian with unit variance in equation 29.

### 3 Trial wave function

The trial wave function is used in both the diffusion and branching algorithms and thus it is important that it be close to the ground state wave function of the system. It also will determine how quickly the calculation converges on the lowest energy of the system. One of the simplest many particle wave functions is an antisymmetrized product of single particle orbitals.

$$\psi_T = \mathcal{A} \prod_{i=1}^A \phi_i(\mathbf{r}_i, s_i) = \frac{1}{A!} \det \phi_i(\mathbf{r}_i, s_i), \tag{30}$$

This is often called a Slater determinant. This wave function represents that long range part of the interactions leaving out short range correlations. The simplest short range correlation that can be formed is Jastrow-like correlation only dependent on space.

$$|\psi_T\rangle = \prod_{i<j} f(r_{ij}) |\phi\rangle \tag{31}$$

This does not include any spin-isospin correlations, and also is not cluster decomposable. A system that obeys cluster decomposition is a system that obeys locality. It manifests itself in the independence of systems that are separated in space. If I take a system of particles



and split the system into two subsystems,  $A$  and  $B$ , that are far apart, the wave function of the physical system would be the product of the two wave functions  $|A + B\rangle = |A\rangle |B\rangle$ . That is because real physical systems are cluster decomposable. A completely uncorrelated Slater determinant is a cluster decomposable wave function. The most general way to include spin-isospin dependent correlations to a Slater determinant, while maintaining the cluster decomposability of the system, is to use an exponential of the correlation operators.

$$|\psi_T\rangle = \prod_{i<j} f_c(r_{ij}) e^{\sum_p f_p(r_{ij}) \mathcal{O}_{ij}^p} |\phi\rangle \quad (32)$$

This is an infinite sum, and is impossible to calculate directly on a computer and so if we then assume that the correlations are small, we can then expand the exponential to first order getting

$$|\psi_T\rangle = \prod_{i<j} f_c(r_{ij}) \left( 1 + \sum_p f_p(r_{ij}) \mathcal{O}_{ij}^p \right) |\phi\rangle. \quad (33)$$

We further expand this and truncate this product to first order, keeping only linear terms in the expansion. To improve this estimation I have included the quadratic terms from this expansion into the calculation, as well as a subset of the quadratic terms called independent pair terms. I'll show this expansion with the example of  $A = 3$  for convenience. Expanding equation 33 we get

$$\begin{aligned} & \left[ f_c(r_{12}) \left( 1 + \sum_p f_p(r_{12}) \mathcal{O}_{12}^p \right) \right] \left[ f_c(r_{13}) \left( 1 + \sum_p f_p(r_{13}) \mathcal{O}_{13}^p \right) \right] \left[ f_c(r_{23}) \left( 1 + \sum_p f_p(r_{23}) \mathcal{O}_{23}^p \right) \right] \\ &= f_c(r_{12}) f_c(r_{13}) f_c(r_{23}) \left( 1 + \sum_p f_p(r_{12}) \mathcal{O}_{12}^p + \sum_p f_p(r_{13}) \mathcal{O}_{13}^p + \sum_p f_p(r_{23}) \mathcal{O}_{23}^p \right. \\ & \quad \left. + \sum_p f_p(r_{12}) \mathcal{O}_{12}^p \sum_q f_q(r_{13}) \mathcal{O}_{13}^q + \sum_p f_p(r_{12}) \mathcal{O}_{12}^p \sum_q f_q(r_{23}) \mathcal{O}_{23}^q + \sum_p f_p(r_{13}) \mathcal{O}_{13}^p \sum_q f_q(r_{23}) \mathcal{O}_{23}^q \right) \\ &= \left[ \prod_{i<j} f_c(r_{ij}) \right] \left[ 1 + \sum_{i<j} \sum_p f_p(r_{ij}) \mathcal{O}_{ij}^p + \frac{1}{2} \sum_{i<j} \sum_p f_p(r_{ij}) \mathcal{O}_{ij}^p \sum_{\substack{k<l \\ ij \neq kl}} \sum_q f_q(r_{kl}) \mathcal{O}_{kl}^q + \dots \right]. \end{aligned} \quad (34)$$

In the example with  $A = 3$  we only get up to triplet terms, of which there is only one, but you can imagine many more terms if you have more particles. With previous calculations we have approximated this by only taking up to the linear term.

$$|\psi_T\rangle = \left[ \prod_{i<j} f_c(r_{ij}) \right] \left[ 1 + \sum_{i<j} \sum_p f_p(r_{ij}) \mathcal{O}_{ij}^p \right] |\phi\rangle. \quad (35)$$

I have included the quadratic correlations above, but I have also done a calculation with a subset of these correlations called independent pair terms. These independent pair terms only include pairs where there is no common particle among the two sets of pairs. Calculations

were done with these independent pairs because we believed that they would capture most of the physics of the quadratic terms.

$$|\psi_T\rangle = \left[ \prod_{i<j} f_c(r_{ij}) \right] \left[ 1 + \sum_{i<j} \sum_p f_p(r_{ij}) \mathcal{O}_{ij}^p \left( 1 + \sum_{k<l, \text{ip}} \sum_q f_q(r_{kl}) \mathcal{O}_{kl}^q \right) \right] |\phi\rangle \quad (36)$$

The sum  $\sum_{k<l, \text{ip}}$  is a sum over all of the  $kl$  pairs that don't have a particle that matches either the  $i^{\text{th}}$  or the  $j^{\text{th}}$  particle. This is the independent pair sum.

## 4 Results

I have calculated binding energies with all three types of correlations, linear, independent pair (IP), and quadratic, and compared the results. In all cases we have used the v6 potential and the same operators for the correlations. In each case the weights for each operator were determined variationally. Calculations were done for systems,  $^4\text{He}$  and  $^{16}\text{O}$  and the binding energies are reported in table 1 with and without IP correlations and compared to the experimental value.

Table 1: Binding energies in MeV for  $^4\text{He}$  and  $^{16}\text{O}$  as calculated with all three types of correlations compared to experimental energies.

	Linear	IndPair	Quadratic	Expt.
$^4\text{He}$	-27.17(4)	-26.33(3)	-25.35(3)	-28.295
$^{16}\text{O}$	-115.7(9)	-121.5(1.5)	-120.0(1.4)	-127.619

I have also calculated the energy per nucleon of symmetric nuclear matter (SNM) with density  $\rho = 0.16\text{fm}^{-3}$  of 28 particles with periodic boundary conditions. The energy per nucleon was -13.92(6) MeV for linear correlations, -14.80(7) MeV for IP correlations, and ??? with the full set of quadratic correlations.

Notice that in the case of  $^{16}\text{O}$  and SNM the IP and quadratic correlations caused the binding energies to decrease, while in the case of  $^4\text{He}$  the binding energy went up when IP correlations were added, and even more when the quadratic correlations were added. We expected the energies and uncertainties to decrease a little for each calculations since we were using a more correct wave function. This was true for  $^{16}\text{O}$  and SNM, but not for  $^4\text{He}$ . The binding energy for  $^4\text{He}$  increased with both new types of correlations. At first I thought that this could be due to the small number of extra terms in the IP correlation with only 4 particles, however the quadratic correlations, which have many more terms, also caused the energy to increase. I'm not yet sure why the energy increased for  $^4\text{He}$ . To determine if this increase was reasonable we did calculations for  $^4\text{He}$  with all three correlations with the constraint removed. The constraint is used to control the fermi-sign problem and when unconstrained calculations are controlled they should converge to the exact answer. We did calculations to see if all three correlation types would converge to the same value. There was evidence that this was the case, but the data became too noisy to be sure. The scaling of the calculations with IP and quadratic correlations in relation to the original linear correlations

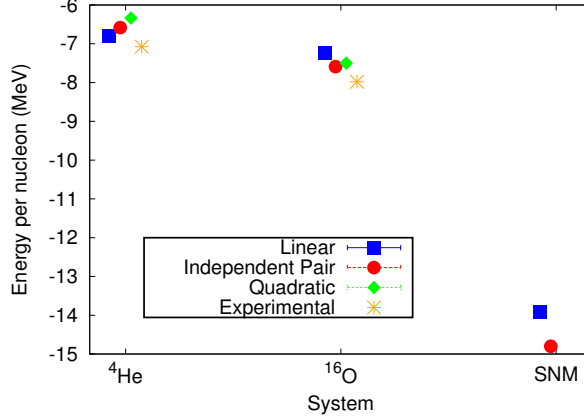


Figure 1: Binding energies per nucleon for  $^4\text{He}$  and  $^{16}\text{O}$  as calculated with linear, independent pair and quadratic correlations. Also, the energy per nucleon of symmetric nuclear matter of 28 particles in a periodic box with density  $\rho = 0.16\text{fm}^{-1}$ . All calculations are compared to their expected values.

is given in figure 2. To calculate the scaling the average time to complete one block of calculations was used.

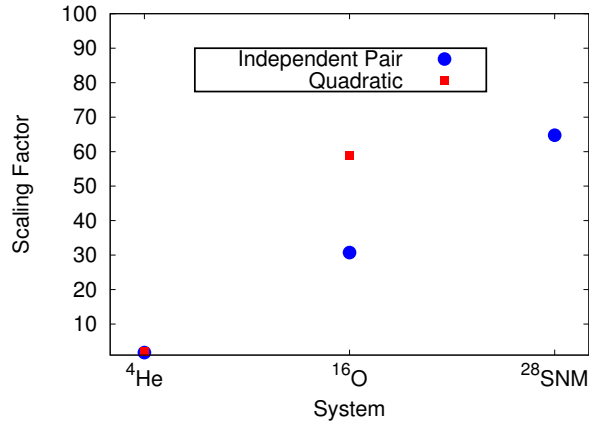


Figure 2: Scaling factors for  $^4\text{He}$ ,  $^{16}\text{O}$  and symmetric nuclear matter as calculated with the average time to complete a block of calculations. The factor is a ratio of the time to calculate the independent pair calculations compared to the time to calculate with the linear correlations. The factors are 3.99, 109.31, and 220.65 respectively.

## 5 Conclusion and Outlook

As mentioned before, one of the most important parts of the calculation is to have a good estimate for the trial wave function that is possible and inexpensive to calculate. So far I have implemented and tested a method for improving the trial wave function used in AFDMC calculation of nuclei and nuclear matter. I have done this by including independent pair

and the full quadratic terms in the correlation operator which currently only has linear terms. The addition of these terms has caused the binding energy of  $^4\text{He}$  to increase and the binding energy of  $^{16}\text{O}$  and SNM to decrease. It is puzzling that the energies for  $^{16}\text{O}$  and SNM decreased by so much. We did not expect the energy of  $^4\text{He}$  to increase with these improved wave functions. To test if this was reasonable we did calculations of  $^4\text{He}$  with all correlation types with the constraint removed, but the data was too noisy to determine if all three correlations converged to the same value.

Another way to improve the trial wave function is to include more terms in the expansion of the exponential correlation operator in equation 32. As we have learned from the IP expansion that we implemented, this would get computationally intractable as the number of particles gets large. Another alternative is to rewrite the correlation operator in terms of a Hubbard-Stratanovich transformation as is done with the spin-isospin dependent part of the propagator in section 2.5. Future work will be done to handle the correlation operators in this way. I will also be searching for additional ways to improve the trial wave function.

With an improved trial wave function I will be using AFDMC to investigate some interesting aspects of nuclear physics and nuclear astrophysics. For example, I will be investigating the formation of deuteron and alpha particle clusters at various densities in mostly neutron matter. Many types of clustering in physics deal with two particles at a time. Alpha particles are thus a special case of four fermion clustering due to the two additional isospin degrees of freedom in addition to the two spin states for spin 1/2 particles. Work has been done to show the light clustering ( $A \leq 4$ ) and condensation of particles in nuclear systems [25, 26, 27] including neutron stars [28, 29, 30]. I plan to show that the AFDMC method, with an improved nuclear wave function can be used to study properties of light clustering in nuclear systems as well. One way I will be doing this will be to do AFDMC calculation with 14 neutrons in a periodic box with the addition of 2 protons at a variety of densities to observe the formation of an alpha particle in neutron matter. Once these clusters are observed with AFDMC the density can be varied to determine the density at which the clusters dissolve as in [29]. This work will be especially applicable to the study of alpha formation in neutron stars.

In conclusion, I have done AFDMC calculations to calculate the binding energy of  $^4\text{He}$  and  $^{16}\text{O}$  as well as the energy per particle of SNM. I have done these calculations with both linear correlation terms, linear plus IP correlations and linear plus all of the quadratic correlations in the trial wave function. We are still trying to understand the increase in energy for  $^4\text{He}$ . In order to maintain the cluster decomposability of the trial wave function, which is lost with either the linear or IP correlations, I will be using the Hubbard-Stratanovich transformation to sample the exponential spin-isospin dependent correlations. This is analagous to the sampling of spin-isospin states in the propagator of AFDMC. I will also be looking for additional ways to improve the trial wave function. I will then be applying these calculations to other interesting nuclear systems such as the clustering of alpha particles in neutron matter.

## References

- [1] J. M. Lattimer and M. Prakash. Neutron star structure and the equation of state. *Astrophys. J.*, 550:426, 2001.
- [2] J. M. Lattimer and M. Prakash. The physics of neutron stars. *Science*, 304:536, 2004.
- [3] J. Rikova Stone, J. C. Miller, R. Koncewicz, P. D. Stevenson, and M. R. Strayer. Nuclear matter and neutron-star properties calculated with the skyrme interaction. *Phys. Rev. C*, 68, 2003.
- [4] F. Douchin and P. Haensel. A unified equation of state of dense matter and neutron star structure. *Astron. Astrophys.*, 380:151, 2001.
- [5] Henning Heiselberg and Vijay Pandharipande. Recent progresses in neutron star theory. *Annu. Rev. Nucl. Part. Sci.*, 50:481, 2000.
- [6] Hideki Yukawa. On the interaction of elementary particles. i. *Proceedings of the Physico-Mathematical Society of Japan. 3rd Series*, 17:48, 1935.
- [7] C. M. G. Lattes, H. Muirhead, G. P. S. Occhialini, and C. F. Powell. Processes involving charged mesons. *Nature*, 159:694–697, 1947.
- [8] Leonard S. Kisslinger and Debasish Das. Review of qcd, quark-gluon plasma, heavy quark hybrids, and heavy quark state production in p-p and a-a collisions. *Int. J. Mod. Phys. A*, 31, 2016.
- [9] Petr Navrátil, Sofia Quaglioni, Ionel Stetcu, and Bruce R Barrett. Recent developments in no-core shell-model calculations. *Journal of Physics G: Nuclear and Particle Physics*, 36(8):083101, 2009.
- [10] Bruce R. Barrett, Petr Navrátil, and James P. Vary. *Ab initio* no core shell model. *Prog. Part. Nucl. Phys.*, 69:131–181, 2013.
- [11] G Hagen, T Papenbrock, M Hjorth-Jensen, and D J Dean. Coupled-cluster computations of atomic nuclei. *Rep. Prog. Phys.*, 77(9):096302, 2014.
- [12] W.H. Dickhoff and C. Barbieri. Self-consistent green’s function method for nuclei and nuclear matter. *Prog. Part. Nucl. Phys.*, 52(2):377 – 496, 2004.
- [13] V. Somà, A. Cipollone, C. Barbieri, P. Navrátil, and T. Duguet. Chiral two- and three-nucleon forces along medium-mass isotope chains. *Phys. Rev. C*, 89:061301, Jun 2014.
- [14] H. Hergert, S.K. Bogner, T.D. Morris, A. Schwenk, and K. Tsukiyama. The in-medium similarity renormalization group: A novel *ab initio* method for nuclei. *Phys. Rep.*, 621:165–222, 2016. Memorial Volume in Honor of Gerald E. Brown.
- [15] J. E. Lynn and K. E. Schmidt. Real-space imaginary-time propagators for non-local nucleon-nucleon potentials. *Phys. Rev. C*, 86:014324, Jul 2012.

- [16] David J. Gross and Frank Wilczek. Ultraviolet behavior of non-abelian gauge theories. *Phys. Rev. Lett.*, 30:1343, 1973.
- [17] H. David Politzer. Reliable perturbative results for strong interactions? *Phys. Rev. Lett.*, 30:1346, 1973.
- [18] J. Carlson, S. Gandolfi, F. Pederiva, Steven C. Pieper, R. Schiavilla, K.E. Schmidt, and R.B. Wiringa. Quantum monte carlo methods for nuclear physics. *Rev. Mod. Phys.*, 87:1067, 2015.
- [19] J. C. Slater. A simplification of the hartree-fock method. *Phys. Rev.*, 81:385, 1951.
- [20] Robert Jastrow. Many-body problem with strong forces. *Phys. Rev.*, 98:1479, 1955.
- [21] M. H. Kalos. Monte carlo calculations of the ground state of three- and four-body nuclei. *Phys. Rev.*, 128:1791, 1962.
- [22] K. E. Schmidt and S. Fantoni. A quantum monte carlo method for nucleon systems. *Phys. Lett. B*, 446:99–103, 1999.
- [23] W. M. C. Foulkes, L. Mitas, R. J. Needs, and G. Rajagopal. Quantum monte carlo simulations of solids. *Rev. Mod. Phys.*, 73:33–83, 2001.
- [24] R.B. Wiringa, R.A. Smith, and T.L. Ainsworth. Nucleon-nucleon potentials with and without  $\Delta(1232)$  degrees of freedom. *Phys. Rev. C*, 29:1207, 1984.
- [25] P. Schuck, Y. Funaki, H. Horiuchi, G. Röpke, A. Tohsaki, and T. Yamada.  $\alpha$ -particle condensation in nuclear systems. *Nucl. Phys. A*, 788:293c–300c, 2007.
- [26] P. Schuck, Y. Funaki, H. Horiuchi, G. Röpke, A. Tohsaki, and T. Yamada. Alpha-particle condensation in nuclear systems. *J. Phys.: Conf. Ser.*, 413:012009, 2013.
- [27] P. Schuck. Alpha-particle condensation in nuclear systems: present status and perspectives. *J. Phys.: Conf. Ser.*, 436:012065, 2013.
- [28] S. S. Avancini, C. C. Barros, D. P. Menezes, and C. Providência.  $\alpha$  particles and the “pasta” phase in nuclear matter. *Phys. Rev. C*, 82:025808, Aug 2010.
- [29] S.S. Avancini, C.C. Barros Jr., L. Brito, S. Chiacchiera, D.P. Menezes, and C. Providência. Light clusters in nuclear matter and the “pasta” phase. *Phys. Rev. C*, 85:035806–1, 2012.
- [30] Ad.R. Raduta, F. Aymard, and F. Gulminelli. Clusterized nuclear matter in the (proto-)neutron star crust and the symmetry energy. *Eur. Phys. J. A*, 50:24, 2014.